Food and Chemical Toxicology 125 (2019) 198–209

Contents lists available at ScienceDirect

Food and Chemical Toxicology

journal homepage: www.elsevier.com/locate/foodchemtox

Carvacrol/β-cyclodextrin inclusion complex inhibits cell proliferation and migration of prostate cancer cells

Gabriela G.G. Trindade[a], Greeshma Thrivikraman[b], Paula P. Menezes[a], Cristiane M. França[b], Bruno S. Lima[a], Yasmim M.B.G. Carvalho[a], Eloísa P.B.S.S. Souza[a], Marcelo C. Duarte[a], Saravanan Shanmugam[a], Lucindo J. Quintans-Júnior[c], Daniel P. Bezerra[d], Luiz E. Bertassoni[b,e,f,g,**], Adriano A.S. Araújo[a,*]

[a] Department of Pharmacy, Federal University of Sergipe, São Cristóvão, Sergipe, Brazil
[b] Division of Biomaterials and Biomechanics, Department of Restorative Dentistry, School of Dentistry, Oregon Health and Science University, Portland, OR, United States
[c] Department of Physiology, Federal University of Sergipe, São Cristóvão, Sergipe, Brazil
[d] Gonçalo Moniz Institute, Oswaldo Cruz Foundation, Salvador, Bahia, Brazil
[e] Department of Biomedical Engineering, Collaborative Life Science Building, Oregon Health and Science University, Portland, OR, United States
[f] Center for Regenerative Medicine, Oregon Health and Science University, Portland, OR, United States
[g] Cancer Early Detection Advanced Research, Knight Cancer Institute, Portland, OR, United States

ARTICLE INFO

Keywords:
Carvacrol
Inclusion complex
β-cyclodextrin
Cell viability
Prostate cancer

ABSTRACT

Carvacrol, a phenolic monoterpene derived from thyme oil has gained wide interest recently because of its anticancer activities. To improve the solubility of carvacrol, the formation of inclusion complexes with β-cyclodextrin was performed by ultrasound and freeze-drying methods and characterized using thermal analysis, FTIR, XRD, SEM, NMR and HPLC analysis. From these results, carvacrol was successfully complexed within β-cyclodextrin cavity. Moreover, HPLC analysis demonstrated a higher entrapment efficiency for freeze-drying method (81.20 ± 0.52%) in contrast to ultrasound method (34.02 ± 0.67%). Hence, freeze-drying inclusion complex was evaluated for its antiproliferative effect and cytotoxicity against prostate cancer cell line (PC3) *in vitro*. Further, freeze-drying complex led to a dose-dependent inhibition in tumor cell growth in 2D and 3D cell culture systems. Altogether, the inclusion of carvacrol in β-cyclodextrin led to the formation of stable complexes with potent antiproliferative effects against PC3 cells, *in vitro*. Such an improved cytotoxic effect can be attributed to the enhanced the aqueous solubility and bioavailability of carvacrol by effective complexation in β-cyclodextrin.

1. Introduction

Prostate cancer represents the second most common cancer in men, accounting for 19% of total cancers in males worldwide (Siegel et al., 2018). In most cases, prostate cancer develops slowly, although aggressive forms also occur. Metastatic tumor sprouting significantly impairs patients survival, and this process can include proliferative, migratory and invasive activities of cancer cells associated with tumor angiogenesis (Ahmad et al., 2017).

Traditional treatments have been accepted to extend the life expectancy of prostate cancer patients, including surgery, radiation and chemotherapy (Felgueiras et al., 2014). However, the therapeutic use of some chemotherapeutic drugs such as paclitaxel, docetaxel, doxorubicin, etoposide, vinblastine, is still very limited and have shown high toxicity, causing severe side effects (Gupta, 2007). Hence, the development of effective prostate cancer treatments remains highly

* Corresponding author. Department of Pharmacy, Federal University of Sergipe, Av. Marechal Rondon, Jardim Rosa Elze, 49100-000, São Cristóvão, Sergipe, Brazil.
** Corresponding author. Department of Restorative Dentistry, School of Dentistry, Oregon Health and Science University, 2730 S.W. Moody Ave, Portland, OR, 97201, USA.
E-mail addresses: gabyggt@gmail.com (G.G.G. Trindade), greeshmatnair@gmail.com (G. Thrivikraman), paula.dp.menezes@gmail.com (P.P. Menezes), cristiane321@gmail.com (C.M. França), brunolimafarm@gmail.com (B.S. Lima), yasmimgomess@gmail.com (Y.M.B.G. Carvalho), eloisaportugal@gmail.com (E.P.B.S.S. Souza), duarte6cavalcante@gmail.com (M.C. Duarte), saranflora04@gmail.com (S. Shanmugam), lucindojr@gmail.com (L.J. Quintans-Júnior), danielpbezerra@gmail.com (D.P. Bezerra), bertasso@ohsu.edu (L.E. Bertassoni), adriasa2001@yahoo.com.br (A.A.S. Araújo).

https://doi.org/10.1016/j.fct.2019.01.003
Received 1 October 2018; Received in revised form 2 December 2018; Accepted 3 January 2019
Available online 04 January 2019
0278-6915/

desirable.

Extensive research has been carried out to develop antitumor therapeutics from natural products derived from plants, due to their ability to interact with the molecular targets in biological system (Iqbal et al., 2017; Kaur et al., 2017). Natural compounds (also called phytochemicals) are biologically active substances present in plants, such as monoterpenes, which can be obtained in the essential oils of aromatic plants (Rejhová et al., 2018). Monoterpenes are shown to be interesting compounds for the development of new drugs for therapy of prostate cancer, such as geraniol (Kim et al., 2011), menthol (Wang et al., 2012), linalool (Zhao et al., 2017), D-limonene (Bishayee and Rabi, 2009) and carvacrol (Luo et al., 2016).

Carvacrol is a phenolic monoterpene found in essential oils of plants belonging to the genera *Origanum* and *Thymus*. Many studies have demonstrated a variety of pharmacological properties, including gastroprotective (Souza et al., 2017), analgesic (Can Baser, 2008), antioxidant (Guimarães et al., 2010), antibacterial (Ben Arfa et al., 2006), anti-inflammatory (Guimarães et al., 2012) and antinociceptive (Melo et al., 2012). In addition, as a novel anticancer agent, carvacrol was reported to have an antiproliferative effect in several types of cancer cells, including lung (Koparal and Zeytinoglu, 2003), liver (Yin et al., 2012), breast (Arunasree, 2010), colon (Fan et al., 2015), stomach (Günes-Bayir et al., 2018) and prostate cell lines (Luo et al., 2016). Accordingly, Chen et al. (2015) demonstrated that carvacrol reduced the viability, migration and invasion of human gioblastoma cells. Dai et al. (2016) also reported the effect of carvacrol in human oral squamous cell carcinoma (OSCC) and showed that it inhibited cell proliferation, metastasis and invasion, and induced apoptosis. More recently, it has been demonstrated that carvacrol significantly inhibited the viability of human prostate cancer cells (Luo et al., 2016). Based upon these studies, it has been postulated that carvacrol may have a broad spectrum of cytotoxic and anticancer activities. However, its low bioavailability due to poor water solubility, high volatility and instability have significantly limited its pharmaceutical application. Based on the potential anticancer effects mentioned above, there is critical need to improve the solubility and bioavailability of carvacrol to enhance its therapeutic potential.

Currently, the inclusion technology of cyclodextrins and water-insoluble drugs has been widely used to enhance both stability and solubility of more hydrophobic drugs, as well as to modify the drug release profile in order to improve the pharmacological properties of these compounds. Moreover, such inclusion process can also eliminate undesired characteristics of certain drugs, such as unpleasant odor and taste (Kurkov and Loftsson, 2013). Cyclodextrins are a class of cyclic oligosaccharides consisting of 6 (α-cyclodextrin), 7 (β-cyclodextrin), 8 (γ-cyclodextrin) or more glucopyranose units linked by α-(1,4) bonds (Del Valle, 2004). Cyclodextrins are derived from starch, are non-toxic and biodegradable under favorable conditions. Their unique physicochemical properties including a hydrophilic external surface and a hydrophobic internal cavity allows for the formation of inclusion complexes with several hydrophobic organic molecules (Kurkov and Loftsson, 2013). Among different cyclodextrins, β-cyclodextrin is widely used due to its suitable cavity size for a wide range of small molecules including the monoterpenes, and has been on the GRAS list since 1998 as a flavor carrier and protectant (Szente and Szejtli, 2004). β-cyclodextrin have been known to be an attractive nano-delivery vehicles due to the development of supramolecular functional materials, as anticancer agent. Gigliotti et al. (2016) reported that, *in vitro* therapeutic effect of camptothecin, a pentacyclic alkaloid, encapsulated in β-cyclodextrin-nanosponges in prostate cancer cells showed that the β-cyclodextrin enhanced inhibition of adhesion and migration of DU145 and PC3 prostate cancer cell lines.

Based on intrinsic properties of cyclodextrins we hypothesized that the formation of carvacrol/β-cyclodextrin complexes could be a promising drug delivery system with enhanced properties such as solubility and anticancer activity. In this research, we investigate an effective method for the preparation of inclusion complexes through their physicochemical characterization by key techniques incorporation. Finally, the most efficient inclusion complex was selected and its inhibitory effect on the proliferation and migration of PC3 cells using 2D and 3D cell culture system *in vitro* was evaluated in this study.

2. Materials and methods

2.1. Materials

Carvacrol (98%, molecular weight 150.22), β-cyclodextrin (≥97%, molecular weight 1135.01) were purchased from Sigma-Aldrich (St. Louis, Missouri, USA). HPLC-grade acetonitrile and deuterated dimethylsuphoxide-d_6 (DMSO-d_6) were purchased from Merck Co., Ltd (Germany). Water used for solutions was purified by Milli-Q system (Millipore). Other reagents were of analytical grade.

2.2. Preparation of inclusion complexes

All samples were prepared in a 1:1 molar ratio of carvacrol to β-cyclodextrin. After processing, samples were stored in a desiccator until submitted for analysis. For physical mixture, an equimolar mixture of carvacrol (150 mg) and β-cyclodextrin (1135 mg) was accurately weighed and tumble-mixed for 15 min. For ultrasound method, β-cyclodextrin (1135 mg) was dissolved in distilled water (100 ml) and carvacrol (150 mg) was dissolved in ethanol (100 ml). Carvacrol solution was then mixed with β-cyclodextrin solution under constant stirring. After ultra-sonicating for 1 h, the organic solvent was removed under vacuum as described by Su et al. (2012). The resulting solution was filtered with a 0.45 μm syringe filter and frozen at −60 °C and subsequently dried for 48 h in a freeze dryer (Labconco FreeZone 4.5, USA). For freeze-drying method, carvacrol was added to the aqueous solution of β-cyclodextrin while constant mixing with a magnetic stirrer. After equilibrating the mixture in an orbital shaker (Quimis Q 261A21, Brazil) operating at 150 rpm at room temperature for 36 h, the resulting solution was frozen at −60 °C and lyophilized at −50 °C under 1.09 Pa for 48 h in a freeze dryer (Kfoury et al., 2016).

2.3. Thermal analysis by DSC and TG/DTG

Differential scanning calorimetry analysis of free carvacrol, β-cyclodextrin, physical mixture, ultrasound and freeze-drying were carried out using a DSC-60 cell (Shimadzu, DSC-60A, USA) calibrated with indium and zinc metals before sample testing. Samples were accurately weighed (~2 mg) and placed in aluminum pans while an empty pan was used as reference. Samples were heated from 25 to 500 °C at a rate of 10 °C min^{-1} under a nitrogen atmosphere (50 ml min^{-1}).

Thermogravimetric analysis of the samples were obtained using a thermogravimetric analyzer (TGA-60, Shimadzu, USA) under nitrogen atmosphere (100 ml min^{-1}). Each sample (3–5 mg) was placed in a platinum crucible and temperature was increased from 25 to 900 °C at a heating rate of 10 °C min^{-1}. Each set of tests were done in triplicate. Further graphs were plotted by Origin Pro 8 software.

2.4. Moisture determination by Karl Fischer method

Moisture contents of the samples were determined using Karl Fischer Titrino Plus KF 870 (Metrohm) using methanol (Fluka) as a titrating solution. Analyses were performed in triplicate.

2.5. Fourier transform infrared spectroscopy (FTIR)

FTIR spectra were recorded using an IRTracer-100 (Shimadzu) Fourier Transform Infrared spectrophotometer at room temperature. Carvacrol samples, β-cyclodextrin, their inclusion complexes were previously ground and mixed thoroughly with KBr. All analyses were

recorded from 500 to 4000 cm^{-1} with a resolution of 4 cm^{-1}.

2.6. X-ray diffraction (XRD)

X-ray diffraction measurements of the samples were recorded using a Rigaku diffractometer. Samples were irradiated with monochromatized CuKα radiation and analyzed over a 2θ angle range 3–40°. The XRD patterns were collected with tube voltage of 40 kV and tube current of 40 mA in a stepwise scan mode ($1 s^{-1}$).

2.7. Scanning electron microscopy (SEM)

Dried samples were mounted on aluminum stubs, coated with a thin layer of gold and visualized with a scanning electron microscope (JSM-6390-LV JEOL) at an accelerated voltage of 12 kV.

2.8. Entrapment efficiency (EE)

To determine inclusion content, the adsorbed oil was extracted from inclusion complexes by washing 0.5 g of sample with 5 ml of acetonitrile for 20 min with stirring as described by Marreto et al. (2008). The resulting solution was centrifuged at 3200 × *g* for 15 min to remove any β-cyclodextrin from the solution, leaving only the active compound. After the extraction process, 10 mg of the residue was dissolved in 10 ml of ACN. Samples were homogenized for 3 min in a vortex and analyzed by HPLC method at the chromatographic conditions described in SI (supplementary information). The *EE* was calculated according to Equation (1):

$$EE\ (\%) = \frac{mass\ of\ recovered\ carvacrol\ in\ inclusion\ complex}{mass\ of\ added\ carvacrol\ in\ inclusion\ complex} \times 100 \quad (1)$$

2.9. Nuclear magnetic resonance (NMR)

^{1}H NMR and 2D nuclear Overhauser effect spectroscopy (NOESY) spectra were recorded with a Varian VNMRS 500 MHz spectrometer. Samples were dissolved in DMSO-d_6 at 298 K in 5-mm tubes. Chemical shifts were shown in ppm with DMSO-d_6 (2.50 ppm) as the internal standard.

2.10. In vitro cytotoxicity

The prostate cancer cell line, PC3 (kindly provided by Dr. Ryan Gordon, OHSU Knight Cancer Research Institute, Portland, Oregon), was utilized to determine the effectiveness of selected inclusion complex in inhibiting tumor cell proliferation and survival. Further, the cells were cultured as per protocol reported in SI. To examine the antiproliferative effect of the complex, PC3 cells were seeded in 96-well plates at a concentration of 1×10^4 cells/well in 200 µl media and grown for 24 h at 37 °C under a humidified atmosphere containing 5% CO_2 prior to the experiment. After incubation overnight, the media was replaced with fresh media containing different concentrations (25–200 µg/ml) of free carvacrol or freeze-drying inclusion complex and (200 µg/ml) of β-cyclodextrin. Control group was replaced with fresh media (RPMI plus 10% FBS). Before and after adding the treatments (0, 24 h and 48 h), representative phase contrast images of cells were taken using a fluorescence microscope (EVOS FL Auto, Life Technologies). A live/dead assay kit (Ready Probes Cell Viability Imaging Kit, Molecular Probes) was used 48 h post treatment in PC3 cells. After treatment, medium was removed and 100 µl of live/dead solution diluted in phosphate buffered saline (PBS) was added to each well according to the manufacturer's instructions and incubated for 15 min. After incubation, images (4x and 10x) were captured using fluorescence microscope. Live and dead cells were counted using ImageJ software based on at least 3 locations of triplicate samples after 48 h. The percentage of viable cells was then calculated according to equation (2). All experiments were performed in triplicate.

$$Cell\ viability\ (\%) = \frac{Live\ cells}{Total\ cells} \times 100 \quad (2)$$

2.11. 3D cell encapsulation and viability assay

In order to evaluate cell behavior and viability in the presence and absence of different concentrations of freeze-drying inclusion complex (100, 200 and 300 µg/ml) in a preclinical model that better mimics the physiologic responses of cells to the drug in 3D, a gelatin methacrylol (GelMA) hydrogel was used. GelMA was synthesized by reacting gelatin with methacrylic anhydride as previously described by (Nichol et al., 2010). For hydrogel preparation, GelMA macromer at concentration of 5% (w/v) was dissolved in Dulbecco's phosphate buffered saline (DPBS, Sigma) using 0.15% (w/v) Irgacure® 2959 (Tokyo Chemical Industries) as the photoinitiator. GelMA hydrogels were polymerized using UV light (320–390 nm) (EXFO Acticure 4000) with a power of 850 mW for 30 s at a distance of 8.5 cm PC3 cells (1.5×10^4 cells/ml) were re-suspended in GelMA hydrogel and 10 µl of the suspension was dispensed on 3-(trimethoxysilyl) propyl methacrylate (TMSPMA) coated glass slides. The samples were compressed to 100 µm thick disks and then photocrosslinked as described previously. The viability of PC3 cells in 5% (w/v) GelMA hydrogels was determined using a live/dead assay kit under a fluorescence microscope. Percentage of viable cells was calculated based on the number of live cells divided by the total cells as described above.

2.12. Statistical analysis

Data analyses were performed using GraphPad Prism 5.0 (GraphPad Prism software Inc., San Diego, CA, USA). Results were evaluated by the geometric means followed by one-way Analysis of Variance (ANOVA) with Tukey post hoc test ($p < 0.05$) was considered statistically significant.

3. Results

3.1. Thermal characterization

All the samples were subjected to DSC and TG/DTG for the investigations of solid-state interactions between oil and β-cyclodextrin and are presented in Fig. 1.

The DSC curve of carvacrol displayed a broad endothermic peak at 141.86 °C (33–169 °C) corresponding to its volatilization ($\Delta H = 292.68\ J\ g^{-1}$). This peak was partially reduced in the physical mixture curve and disappeared in the ultra-sonicating and freeze-drying inclusion complexes curves. DSC curve of physical mixture is very similar to that β-cyclodextrin, indicating the presence of β-cyclodextrin in free form, with the carvacrol adhered onto the surface. On the other hand, DSC curves of both inclusion methods indicated a clear difference compared to free carvacrol and physical mixture curves, with distinct endothermic events followed by thermal decomposition. The events namely: 30–134 °C ($\Delta H = 240.02\ J\ g^{-1}$ and $184.35\ J\ g^{-1}$, respectively), correspond to the release of water molecules of β-cyclodextrin as well as the release of carvacrol, adsorbed on the surface; a subtle peak at 220–230 °C ($\Delta H = 4.64\ J\ g^{-1}$ and $0.52\ J\ g^{-1}$), which is attributed to the release of encapsulated oil. The last peak occurred in the range of 280–362 °C ($\Delta H = 459.97\ J\ g^{-1}$ and $417.10\ J\ g^{-1}$), which corresponds to fusion followed by decomposition of β-cyclodextrin.

Fig. 1B shows TG/DTG curves of samples and Table 1 lists mass losses calculated from specific intervals for each material analyzed. The carvacrol curve showed a single step weight loss between 32 and 169 °C ($\Delta m = 99.92\%$), which corresponds to the volatilization of monoterpene, as discussed for the DSC analysis. TG/DTG curves of β-

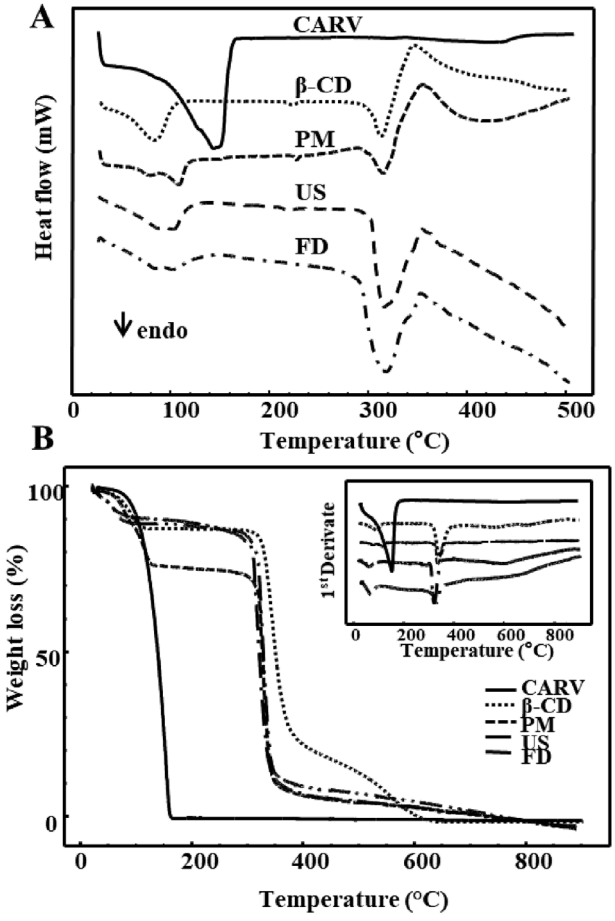

Fig. 1. DSC (A) and TG/DTG (B) curves of carvacrol (CARV), β-cyclodextrin (β-CD), physical mixture (PM), ultrasound (US) and freeze-drying (FD) in dynamic nitrogen atmosphere and heat rate of 10 °C min^{-1}.

cyclodextrin can be divided into four consecutive mass loss steps (1st – evaporation; 2nd – crystalline phase transition; 3rd – melting/degradation and 4th – carbonization), as demonstrated in Table 1.

Similar to the observation made from DSC analysis, TG/DTG curves of physical mixture showed a superposition of the individual components, suggesting a low interaction between carvacrol and β-cyclodextrin. As shown in Table 1, the 1st and 2nd weight loss percentages of ultrasound and freeze-drying inclusion complexes can be attributed to release of complexed carvacrol, since the free oil and β-cyclodextrin had no significant mass loss at this step.

Table 1 shows also the percentages of water content in samples determined by Karl Fischer method. It was observed that there was a reduction of 5.13% of water content when compared to the β-cyclodextrin (13.42 ± 0.6%) and freeze-drying (8.29 ± 0.03%). This difference can be explained as a result of the formation of complexes. Furthermore, it can be seen that the physical mixture method presented the highest weight loss (water and oil) in the first step, because the

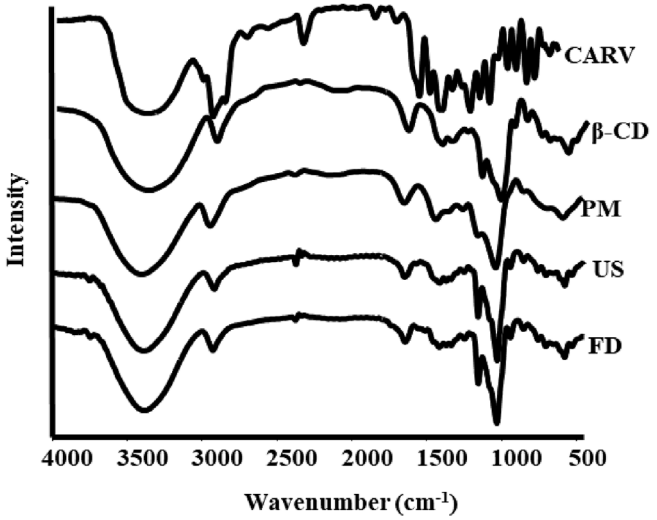

Fig. 2. FTIR spectra of carvacrol, β-cyclodextrin, physical mixture, ultrasound and freeze-drying obtained in the spectral range 4000-500 cm^{-1} in KBr pellets at room temperature.

carvacrol did not form inclusion complexes and remained adhered to the surface of β-cyclodextrin.

3.2. Fourier transform infrared spectroscopy

FTIR spectra of samples were presented in Fig. 2. The IR spectrum of carvacrol showed the presence of the characteristic bands at 3500-3300 cm^{-1} corresponding to stretching vibrations of phenolic O—H group. It was also observed that the intense peaks at 1627 cm^{-1} corresponds to the presence of aromatic C=C stretching vibrations. Moreover, presence of a peak at 1360 cm^{-1} corresponds to the isopropyl group and a strong band in 1250 cm^{-1} is due to C—O stretching vibration. A peak that corresponds to aromatic C—H bending was present at 800-cm^{-1} region, which can be attributed to aromatic ring substitution.

The infrared absorption of β-cyclodextrin exhibited a broad band at 3341 cm^{-1} corresponding to O—H stretching vibrations of the different hydroxyl groups and the band at 1647 cm^{-1} is also related to the O—H groups. The band in the region 1000-700 cm^{-1} corresponds to C—H bonds vibrations and C—C skeleton vibrations related to the glucopyranose ring. The FTIR spectrum of the physical mixture showed approximate superimposition of individual patterns of carvacrol and β-cyclodextrin. The majority of carvacrol prominent absorption bands were covered by that β-cyclodextrin. FTIR spectra of the inclusion complexes showed that carvacrol bands were obscured by very intense and broad β-cyclodextrin bands. However, the absorption bands at 1627 cm^{-1}, 1360 cm^{-1}, 1250 cm^{-1} and 811 cm^{-1} of carvacrol were shifted and decreased in intensity.

3.3. X-ray diffraction (XRD)

Fig. 3 shows the diffraction patterns of samples. β-cyclodextrin

Table 1
Mass loss percentages of carvacrol, β-cyclodextrin, physical mixture, ultrasound and freeze-drying in different temperature intervals obtained by TG/DTG analyses. Water percentages in the samples calculated by Karl Fischer method.

Samples	1st step/% 32–169 °C	2nd step/% 169–290 °C	3rd step/% 290–500 °C	4th step/% 500–900 °C	% H_2O
CARV	99.82 ± 0.07	0.09 ± 0.04	0.24 ± 0.02	0.55 ± 0.01	0.18 ± 0.03
β-CD	13.86 ± 0.31	0.61 ± 0.14	73.30 ± 0.25	14.68 ± 0.08	13.42 ± 0.6
PM	14.26 ± 0.53	1.91 ± 0.06	70.20 ± 0.03	12.31 ± 0.33	14.59 ± 0.51
US	8.71 ± 0.22	3.66 ± 0.24	77.42 ± 0.21	10.74 ± 0.05	12.78 ± 0.16
FD	7.56 ± 0.08	7.27 ± 0.16	78.51 ± 0.04	7.46 ± 0.02	8.29 ± 0.03

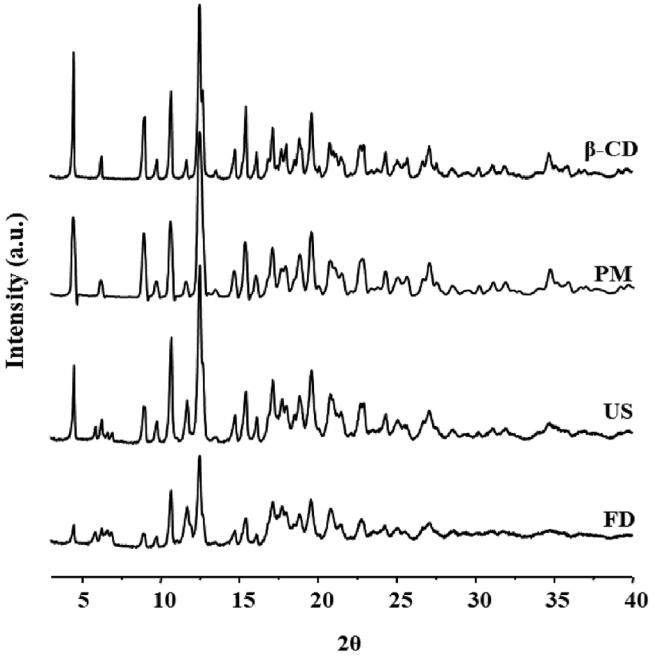

Fig. 3. X-ray diffraction patterns of β-cyclodextrin, physical mixture, ultrasound and freeze-drying.

exhibited many crystalline peaks between 3° and 40° (2θ = 4.38, 6.17, 9.77, 10.7, 12.46 and 23.1°) indicating that β-cyclodextrin mainly existed in a crystalline form. The physical mixture sample also exhibited several characteristic peaks attributable to crystalline β-cyclodextrin (2θ = 4.35, 6.22, 9.82, 10.66, 12.33 and 23.71°) with only a slight decrease in peak intensity. On the other hand, the patterns of ultrasound and freeze-drying inclusion complexes showed some differences, especially the absence of peaks at 4.38° and 6.17° and the appearance of new peaks at 5.79° and 6.82°. In addition, the freeze-drying complex had a comparatively lower degree of crystallinity and presented new solid crystalline phases in the XRD diffractogram.

3.4. Scanning electron microscopy (SEM)

In order to assess the morphological aspects of solid-state carvacrol/β-cyclodextrin system formed, SEM imaging was performed. As shown in Fig. 4, surface morphology of β-cyclodextrin appeared as crystalline particles of irregular/different sizes that are roughly rectangular-shaped. SEM images showed that both structure and shape of physical mixture and inclusion complexes were different, particularly in the ultrasound method, wherein the complex can be observed as small particles or needle-shaped crystals. On the other hand, the particle shapes and morphologies of the physical mixture presented similar characteristics as the particles of β-cyclodextrin. SEM images of freeze-drying inclusion complex appeared as compact and homogeneous plate-like structures, revealing a strong interaction between carvacrol and β-cyclodextrin in the solid state.

3.5. Entrapment efficiency (EE)

A more precise method for evaluation of the solubilizing effects of cyclodextrins is to determine their entrapment efficiency. Fig. S-1 shows the chromatogram of carvacrol with UV absorption spectra at 274 nm and retention time of 5.8 min obtained after the development of the analytical method by HPLC.

The entrapment efficiency of samples were calculated using Eq. (1) and are listed in Table 2. EE values for ultrasound and freeze-drying showed statistically significant differences ($p < 0.05$). The highest percentage of EE was obtained for freeze-drying method with value of 81.20 ± 0.52%; and the lowest EE was obtained for physical mixture (1.15%). Ultrasound method showed a lower (34.02 ± 0.67%) entrapment efficiency than freeze-drying method.

3.6. ^1H and 2D NMR analyses

After resultant EE, free carvacrol and freeze-drying complex were analyzed with ^1H NMR spectroscopy. As shown in Fig. 5, the complex showed the characteristics peaks of protons of both β-cyclodextrin and carvacrol. NMR spectra of carvacrol showed the characteristic peaks of H-1 protons at δ 1.15, H-3 protons at δ 6.92 and H-4 protons at δ 6.65 ppm. After complexation with β-cyclodextrin, these peaks appeared at δ 1.19, δ 6.81 and δ 6.58 ppm, respectively. From Table 3, the results suggested that H-3 (Δδ) and H-4 protons (Δδ) presented higher shift as compared to H-1 protons (Δδ).

3.7. Freeze-drying complex reduces PC3 cell viability and proliferation

After verifying that freeze-drying is the optimal method for the successful inclusion of carvacrol into β-cyclodextrin, we compared their cytotoxic effect on PC3 cells *in vitro*. Cells untreated or treated with β-cyclodextrin (200 μg/ml) were used as controls for carvacrol and complex, respectively. As shown in Fig. 6, images obtained from three independent experiments clearly demonstrated concentration-dependent increase in cytotoxicity treated cancer cells. As expected, inclusion complexes at concentrations as low as 100 μg/ml caused more than 95 ± 0.89% cell death after 48 h of treatment showing significantly higher toxicity than free carvacrol (35.27 ± 1.63%).

PC3 cells treated with β-cyclodextrin (200 μg/ml) as a control group did not show any significant effect on cell viability ($p > 0.05$) which indicates no cytotoxicity of β-cyclodextrin in these cells even at higher concentrations tested. Especially, the results obtained from the live/dead analysis showed 94.7 ± 2.5% live cells after 48 h of treatment with cyclodextrin molecule.

At the lowest tested concentration (25 μg/ml), free oil did not exhibit any significant cytotoxicity to the cancer cells. Cell viability was calculated to be 88.9 ± 2.16% for free carvacrol, which was closer to the percentage viability of control cells (91.5 ± 2.01%) after 48 h while the complex significantly reduced the cell viability at the same concentration, with just 65.90 ± 3.06% live cells ($p < 0.001$).

3.8. Freeze-drying complex inhibits cell migration in vitro

In order to further investigate the inhibitory effect of freeze-drying complex on PC3 cell migration, we performed the scratch assay for 96 h. A linear scratch was made on a confluent monolayer of PC3 cells, which were then cultured with or without increasing concentrations of freeze-drying inclusion complex. Gap distance was measured every 24 h and then compared with the initial gap width at 0 h. As shown in Fig. 7A, it can be clearly observed that cell migration was inhibited in a dose-dependent manner by freeze-drying complex. After 48 h and 96 h, gap closures in control group was 49.47 ± 0.74% and 96.19 ± 0.52%, respectively. In contrast, the results revealed that treatment of PC3 cells after 48 h and 96 h with freeze-drying complex at 200 μg/ml significantly inhibited cell migration (4.96% ± 0.62) compared to control group ($p < 0.001$), as shown in Fig. 7B.

3.9. Cytotoxicity assessment in 3D GelMA hydrogel system

Three-dimensional cell culture systems are known to better reflect physiological cell growth as well as morphology and cell-cell interactions. As shown in Fig. 8, PC3 cells encapsulated in GelMA hydrogels displayed significantly lower cell viability in a dose-dependent manner. Representative fluorescent images of cells cultured *in vitro* are shown in Fig. 8A.

Fig. 8B shows significantly higher toxicity of inclusion complex at

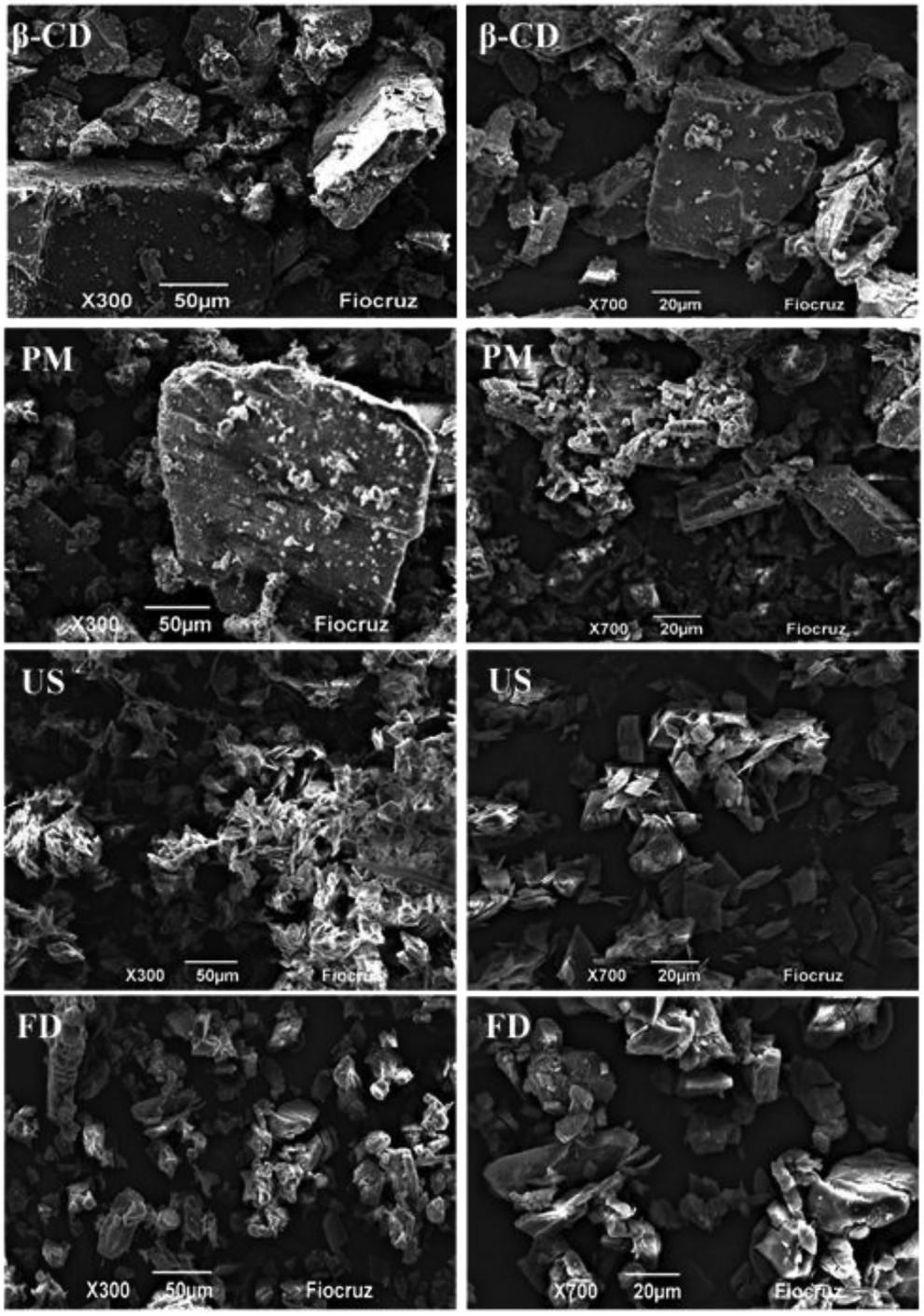

Fig. 4. SEM images of cross-sections (×300 and ×700) of β-cyclodextrin, physical mixture, ultrasound and freeze-drying.

Table 2
Entrapment efficiency (EE) values of carvacrol/β-cyclodextrin inclusion complexes.

Samples	EE (%)*
PM	1.15 ± 0.21
US	34.02^{a} ± 0.67
FD	81.20^{b} ± 0.52

*Values given are averages of three replicate samples; standard deviations are displayed. Entrapment efficiency values with differing superscript letters indicate significantly different values ($p < 0.05$).

higher concentrations tested (300 μg/ml), indicating that more than 90.8 ± 2.3% of the cells were dead after 48 h of treatment with inclusion complex. On the other hand, untreated cells (control group) showed a cell viability of 99.1 ± 0.36%.

4. Discussion

The formation of inclusion complexes using cyclodextrins rely on the interaction between their hydrophobic internal cavity and non-polar or low-polar drugs. Many studies have demonstrated that binding of these molecules to the β-cyclodextrin cavity improves bioavailability of the component and consequently increases biological activity of

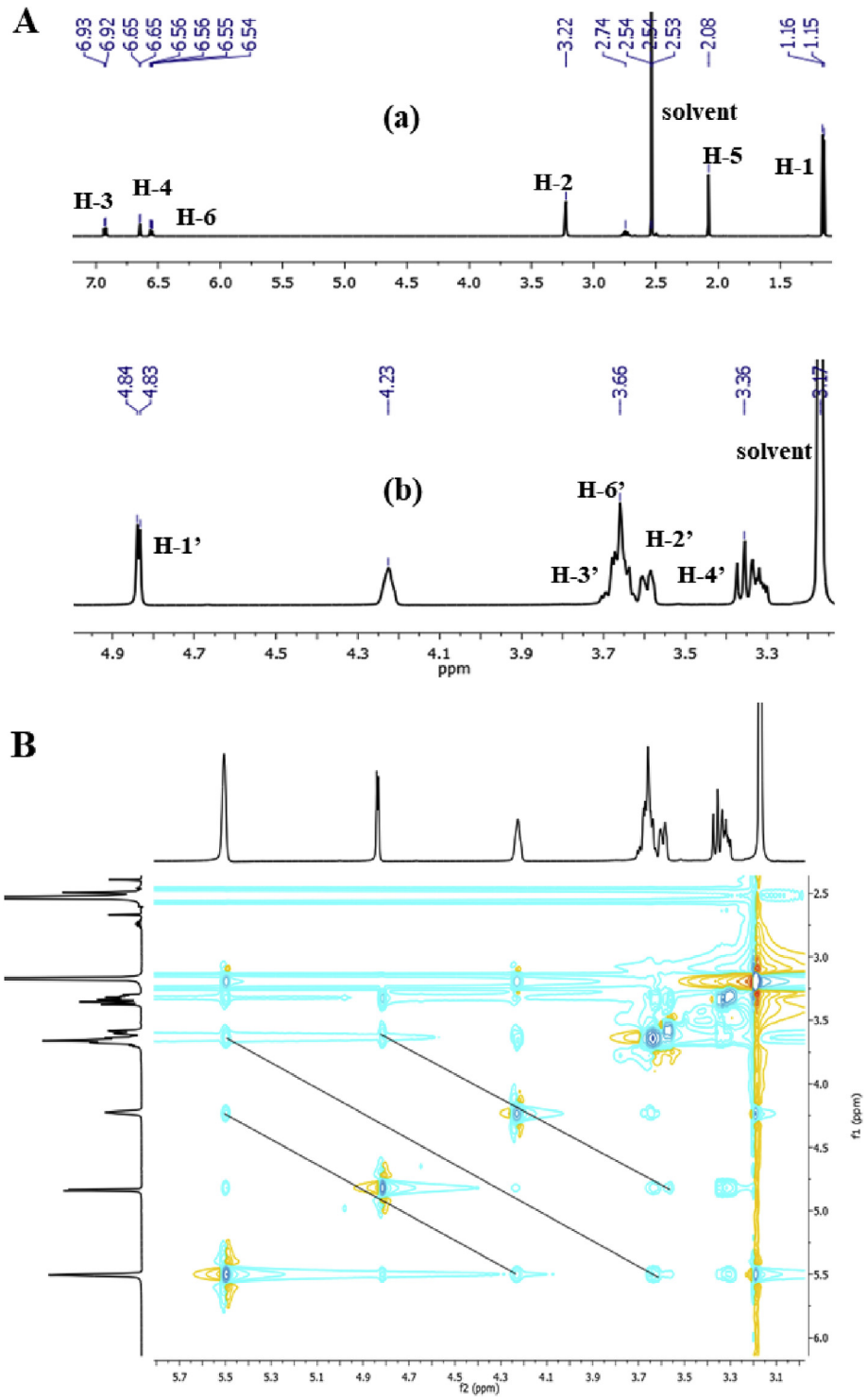

Fig. 5. ^{1}H NMR spectra (A) of free carvacrol (a) and freeze-drying inclusion complex (b) and the 2D NOESY (B) of the inclusion complex in DMSO-d_6.

these drugs. In the present study, inclusion complexation of carvacrol with β-cyclodextrin was performed in order to improve its bioavailability and water solubility that resulted in a marked cytotoxic effect in PC3 cells, due to the release of monoterpene from β-cyclodextrin cavity.

Thermal analyses are extensively used to evaluate solid-state interactions between drugs and cyclodextrins, because of its ability to provide detailed data about both their physical and energetic properties (Mura, 2015). In the DSC analyzes (Fig. 1A), the samples obtained by ultrasound and freeze-drying methods, presented reduction in the intensity of dehydration event related to β-cyclodextrin, probably due to the substitution of water molecules of the β-cyclodextrin cavity by inclusion of monoterpene since the main driving force of complex formation is the release of enthalpy-rich water molecules from this cavity. This happens to favor an apolar-apolar association and a decrease in β-cyclodextrin ring strain, resulting in a more stable lower energy state. Regarding the freeze-drying curves, differences mainly related to the reduction of dehydration event and disappearance of event related to crystalline phase transition of β-cyclodextrin can be explained by an increase in the hydrophobic interactions as carvacrol inserts itself into the apolar β-cyclodextrin cavity by this method, which changes the

Table 3
Chemical shift (δ, ppm) change values relating to the signals of free carvacrol and freeze-drying inclusion complex.

Protons	Free	Inclusion complex	Δδ
H-1	1.15	1.19	0.04
H-2	3.22	3.27	0.05
H-3	6.92	6.81	−0.11
H-4	6.65	6.58	−0.07
H-5	2.08	2.09	0.01
H-6	6.56	6.54	0.02

thermal profile of the new structure formed.

From our TG/DTG results (Table 1), the freeze-drying curve presented an acute mass loss event (169–290 °C), which gives a strong indication of carvacrol inclusion, in contrast to that observed by ultrasound method. This data corroborates with the results of the DSC study. For freeze-drying inclusion complex, 7.27% further mass loss was detected due to the release of carvacrol from its inclusion complex. These results are consistent with the findings reported by Guimarães et al. (2015) and Yildiz et al. (2018) who explained the presence of second degradation step as a result of strong carvacrol encapsulation within the cavity. Furthermore, in order to assess the moisture content of samples, we followed the Karl Fischer technique (Table 1). This technique is a better tool to evaluate water concentration in cyclodextrins and inclusion complexes (Hădărugă, 2012). Our results demonstrated a decrease in water content in complexes formed either by physical mixture or freeze drying method, since water molecules originally found in the cavity of β-cyclodextrin were replaced by carvacrol molecules, during complex formation. Altogether, results from TG/DTA and Karl Fischer suggest better complexation of carvacrol via freeze drying method.

In parallel, we performed infrared spectroscopy, which is a structural elucidation tool widely used for confirmatory analysis of inclusion complexes. This technique allowed identification of all the characteristic peaks of β-cyclodextrin along with few peaks of the ligands that occurred with lower intensity but were found to be shifted at different wavenumber, as shown in Fig. 2. In this way, formation of stable inclusion complexes by freeze-drying method were confirmed by observing the modifications in peak shape, position and intensity. These changes may be related to the formation of intermolecular hydrogen bonds between carvacrol and β-cyclodextrin, which is in accordance with our results of entrapment efficiency. Oliveira et al. (2016) and Santos et al. (2016) also reported changes on the characteristic peaks for α-terpineol and citronellal molecules, respectively, in the spectra of inclusion complexes and identified that monoterpenes were buried inside the cavity of β-cyclodextrin molecule upon inclusion complex formation.

X-Ray diffraction analysis is also considered a simple and efficient method and has been used to analyze crystalline and amorphous nature of the drug and drug-cyclodextrin inclusion complexes. When an inclusion complex is formed, the diffraction patterns of the complexes should be distinct from those of superimposition of individual components. Because of the liquid state, there is no crystallinity of carvacrol in room temperature. The presence of β-cyclodextrin characteristic peaks with reduced intensity in physical mixture and ultrasound methods indicates incomplete inclusion phenomenon (Fig. 3). On the other hand freeze-drying inclusion complex showed undefined, broad and diffuse

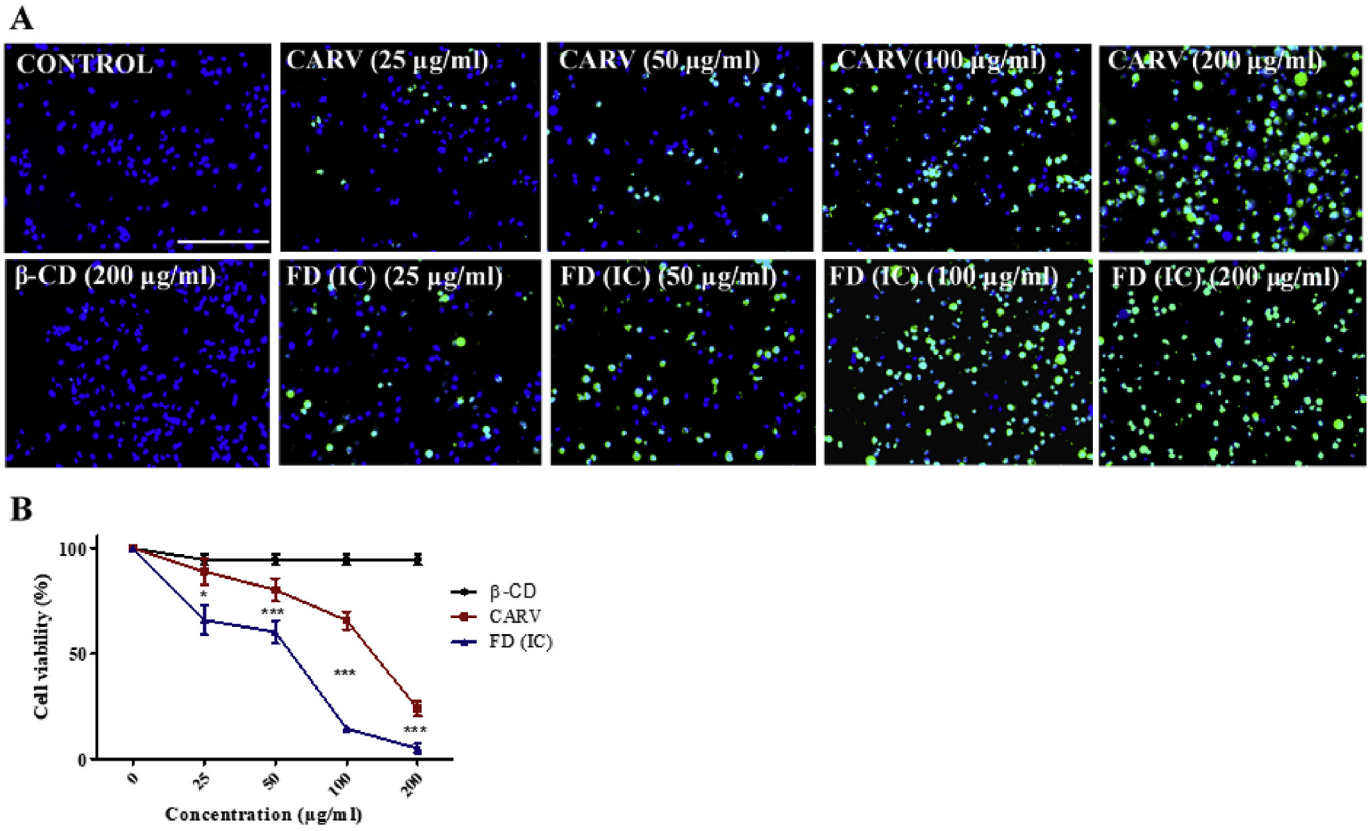

Fig. 6. Freeze-drying inclusion complex (FD (IC)) treatment reduced cell proliferation in prostate cancer cells. Prostate cancer cells (PC3) were treated with different concentrations of free carvacrol and FD (IC) (25, 50, 100, 200 µg/ml) for 48 h. Cells untreated or treated with β-CD (200 µg/ml) were used as controls for carvacrol and FD (IC), respectively. (A) Live/dead assay on PC3 cells was performed after 48 h and fluorescent images from four random fields were captured and were displayed with equal pixel intensity. (B) Quantitative data for cell viability was determined by live/dead assay and data represent mean ± SD of 6 repeats of each treatment group and are expressed as percentage of control group. * ($p < 0.05$), *** ($p < 0.001$) as compared to untreated control values. Scale bar = 400 µm.

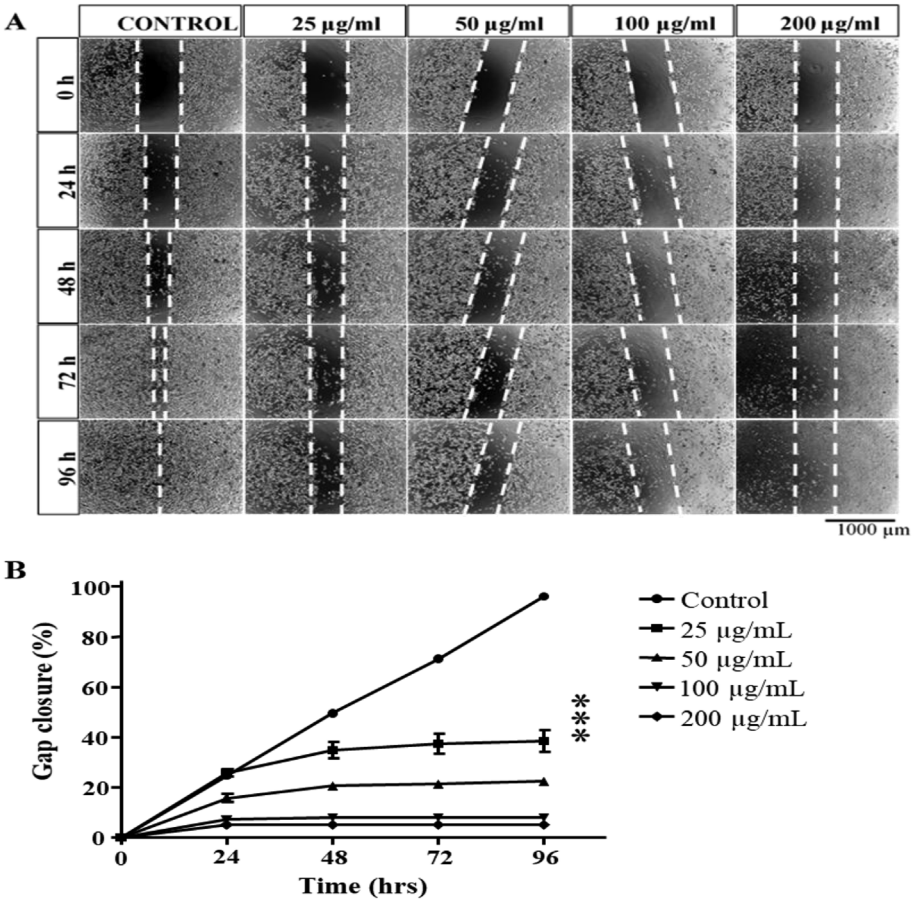

Fig. 7. Effect of inclusion complex on motility of PC3 cells assessed by migration assay. (A) A scratch was made through the PC3 cell layer and then cells were cultured in the presence (25, 50, 100 and 200 µg/ml) and absence of IC for 96 h. Representative images of migration assay were captured immediately after the scratch (0 h) and at 24, 48, 72, and 96 h later, and gap closure (area between the two dotted lines) was analyzed (n = 3). All images were taken at the same scale with a scale bar of 1000 µm. (B) Freeze-drying inclusion complex inhibited PC3 cell migration. The gap closure of freeze-drying treatment group at 24, 48, 72 and 96 h was significantly different compared to the control group at the corresponding time point (***, $p < 0.001$, one-way ANOVA with Tukey post-test, n = 6).

peaks of low intensities that indicates the formation of a significant amount of amorphous material and increase of solubility of sample due to its amorphous nature. Further, appearance of new low intense peaks indicates the change in β-cyclodextrin environment after inclusion complexation.

As shown in Fig. 4, SEM image of freeze-drying showed the presence of rectangular-shaped homogeneous particles, indicating formation of a single solid phase, and consequently, allowing the confirmation of the formation of an inclusion complex due to a strong interaction between oil and cyclodextrin, further supporting the results of DSC, TG/DTG, FTIR and XRD studies.

The hydrophobic interior of the carvacrol/β-cyclodextrin inclusion complex provided the entrapment capacity for carvacrol due to the hydrophobic interaction between the compounds. The entrapment efficiency is a quantitative parameter widely used when characterizing cyclodextrins (Menezes et al., 2016; Wang et al., 2014) and some factors may affect their value, such as β-cyclodextrin intramolecular water content, guest concentration, guest composition, the method used to dry the formed ICs, and the type of solvent used to extract the guest from the β-cyclodextrin. The higher EE was obtained by freeze-drying method (Table 2), which presented EE higher than the thymol/β-cyclodextrin inclusion complex prepared by Dou et al. (2018), but lower than that results prepared by Santos et al. (2015) and Hill et al. (2013) who reported an entrapment efficiency of around 90% for the carvacrol/β-cyclodextrin and eugenol/β-cyclodextrin complexes respectively, with 1:1 ratio obtained also by freeze-drying method. This difference could be attributed to the loss of carvacrol linked to the water that was removed from the β-cyclodextrin cavity during the sublimation process. However, this method was more efficient and contributed to the maximum amount of carvacrol released to support their antiproliferative effects on PC3 cells. NMR results confirmed the formation of inclusion complexes by freeze-drying system. It can be explained based on the orientation of protons. H-3 and H-5 protons are present in the inner surface of β-cyclodextrin and interact more with oil molecules present in its cavity than H-1 protons that are present on the outer surface of β-cyclodextrin cavity. 2D NOESY spectrum of freeze-drying inclusion complex (Fig. 5B) showed considerable correlation of H-3 and H-4 protons of carvacrol with H-3', H-5' protons of β-cyclodextrin. These results indicated that carvacrol were included into β-cyclodextrin cavity.

A key characteristic of most cancers including prostate cancer is an uncontrolled cellular growth, which is highly related to cell motility, and invasiveness. Our cell viability and proliferation assays shows the effect of free carvacrol and the freeze-drying inclusion complex on the cellular survival and proliferation. The dose response curve presented in Fig. 6B showed that the inclusion complex significantly reduced the PC3 cell viability when compared to free carvacrol, indicating that it may have potential in prostate cancer treatment. It is noteworthy that this happens due to the higher solubility of carvacrol in system, revealing its enhanced antiproliferative activity. Given that polyphenols and monoterpenes are known to inhibit cancer-related processes, including prostate cancer, we obtained optimized inclusion complex with carvacrol, a phenolic monoterpene widely used as antiproliferative agent.

As mentioned previously, the supramolecular chemistry of β-cyclodextrin allows water soluble inclusion complex formation with different drug molecules, including anticancer chemotherapeutic agents. Yallapu et al. (2010) developed and characterized β-cyclodextrin-curcumin inclusion complexes by different physiochemical techniques and demonstrated that this carrier system improved curcumin delivery and its antiproliferative effect in prostate cancer cells compared to free curcumin. Our data extends the results of previous investigators

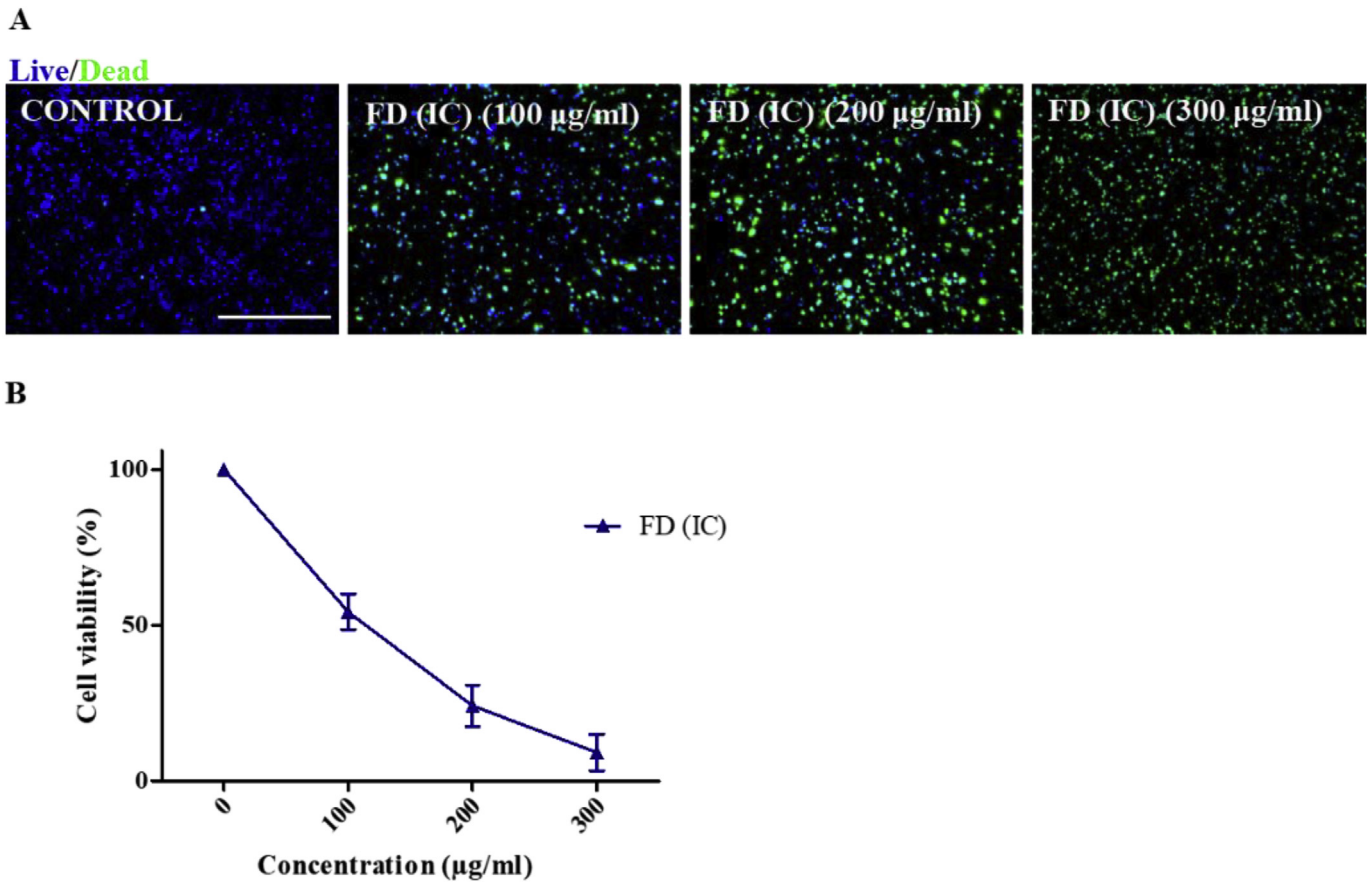

Fig. 8. Effect of inclusion complex on motility of PC3 cells assessed by migration assay. (A) A scratch was made through the PC3 cell layer and then cells were cultured in the presence (25, 50, 100 and 200 µg/mL) and absence of IC for 96 h. Representative images of migration assay were captured immediately after the scratch (0 h) and at 24, 48, 72, and 96 h later, and gap closure (area between the two dotted lines) was analyzed (n = 3). All images were taken at the same scale with a scale bar of 1000 µm. (B) Freeze-drying inclusion complex inhibited PC3 cell migration. The gap closure of freeze-drying treatment group at 24, 48, 72 and 96 h was significantly different compared to the control group at the corresponding time point (***, $p < 0.001$, one-way ANOVA with Tukey post-test, n = 6).

demonstrating that natural products, which are rich in phenolic compounds, associated with β-cyclodextrin, inhibit the cellular growth and migration of human prostate cancer cells.

Cell migration is involved in tumor invasion, metastasis and angiogenesis. The capacity to migrate and invade foreign tissues is a common feature of cancer cells, dramatically contributing to the malignancy of the disease. Thus, after confirming the cytotoxic potential effect of freeze-drying complex, we evaluated PC3 cells motility. Microscopic analysis (Fig. 7) evaluating cell migration into the scratch area at different times showed that in the absence of freeze-drying inclusion complexes, substantial counts of migrating cells were detectable after 48 h, and the gap closure increased significantly. On the other hand, the anti-migration activity of freeze-drying inclusion complex was ascribable to its cytotoxicity, since the concentration used in the migration assay did affect cell viability in the time span of our experiments. However, it is evident that the inclusion complex inhibited migration of cells to a greater extent compared to free carvacrol. Our results are in agreement with Gigliotti et al. (2016) which demonstrated that β-cyclodextrin-nanosponges inhibited the migration of DU145 and PC3 prostate cancer cell lines.

Cell-based assays have been widely used in drug discovery for several decades. 3D cell cultures are well documented to reproduce intrinsic properties and better mimic conditions *in vivo*. Here, we utilized GelMA hydrogel system that has been extensively used for tissue engineering and disease model applications due to its similarity to the native extracellular matrix, and its physical tenability. Further, we had to increase the concentration 3 times to achieve maximum cytotoxicity, since the cells were densely packed in a 3D network. Our data revealed that only the higher concentrations of inclusion complex were able to inhibit the cell viability of PC3 cells encapsulated in this biomaterial. Thus, freeze-drying inclusion complex improved carvacrol physicochemical properties, such as solubility, and significantly reducing cell viability on PC3 cancer cells encapsulated in 3D microenvironments.

5. Conclusions

In this study, we have demonstrated that carvacrol can be successfully complexed with β-cyclodextrin. The inclusion complex formation was confirmed by thermal, spectral, X-ray diffraction and microscopic studies. Our results showed that carvacrol was efficiently entrapped in β-cyclodextrin cavity by freeze-drying method. Freeze-drying inclusion complex effectively reduced cell viability and proliferation of PC3 cells compared to free carvacrol. Additionally, this formulation inhibited the PC3 cell migration. These findings support our hypothesis that β-cyclodextrin enhances the solubility and bioavailability properties of carvacrol, and consequently, their anticancer effects on prostate cancer cells by affecting their viability and migration.

Conflicts of interest

The authors have declared that there is no conflict of interest.

Acknowledgements

We wish to acknowledge Dr. Ryan Gordon (OHSU Knight Cancer Research Institute, Portland, Oregon) for PC3 cells. We also thank the

CAPES (grant numbers 88881.134368/2016-01 and 88881.134337/2016–01), CNPq and FAPITEC/SE for financial support.

Transparency document

Transparency document related to this article can be found online at https://doi.org/10.1016/j.fct.2019.01.003.

Appendix A. Supplementary data

Supplementary data to this article can be found online at https://doi.org/10.1016/j.fct.2019.01.003.

References

Ahmad, G., El Sadda, R., Botchkina, G., Ojima, I., Egan, J., Amiji, M., 2017. Nanoemulsion formulation of a novel taxoid DHA-SBT-1214 inhibits prostate cancer stem cell-induced tumor growth. Cancer Lett. 406, 71–80. https://doi.org/10.1016/j.canlet.2017.08.004.

Arunasree, K.M., 2010. Anti-proliferative effects of carvacrol on a human metastatic breast cancer cell line, MDA-MB 231. Phytomedicine 17, 581–588. https://doi.org/10.1016/j.phymed.2009.12.008.

Ben Arfa, A., Combes, S., Preziosi-Belloy, L., Gontard, N., Chalier, P., 2006. Antimicrobial activity of carvacrol related to its chemical structure. Lett. Appl. Microbiol. 43, 149–154. https://doi.org/10.1111/j.1472-765X.2006.01938.x.

Bishayee, A., Rabi, T., 2009. *d* -Limonene sensitizes docetaxel-induced cytotoxicity in human prostate cancer cells: Generation of reactive oxygen species and induction of apoptosis. J. Carcinog. 8, 1–9. https://doi.org/10.4103/1477-3163.51368.

Can Baser, K., 2008. Biological and pharmacological activities of carvacrol and carvacrol bearing essential oils. Curr. Pharmaceut. Des. 14, 3106–3119. https://doi.org/10.2174/138161208786404227.

Chen, W.-L., Barszczyk, A., Turlova, E., Deurloo, M., Liu, B., Yang, B.B., Rutka, J.T., Feng, Z.-P., Sun, H.-S., 2015. Inhibition of TRPM7 by carvacrol suppresses glioblastoma cell proliferation, migration and invasion. Oncotarget 6, 16321–16340. https://doi.org/10.18632/oncotarget.3872.

Dai, W., Changfu, S., Shaohui, H., Qing, Z., 2016. Carvacrol suppresses proliferation and invasion in human oral squamous cell carcinoma. OncoTargets Ther. 9, 2297–2304. https://doi.org/10.2147/OTT.S98875.

Del Valle, E.M.M., 2004. Cyclodextrins and their uses: A review. Process Biochem. 39, 1033–1046. https://doi.org/10.1016/S0032-9592(03)00258-9.

Dou, S., Ouyang, Q., You, K., Qian, J., Tao, N., 2018. An inclusion complex of thymol into β-cyclodextrin and its antifungal activity against *Geotrichum citri-aurantii*. Postharvest Biol. Technol. 138, 31–36. https://doi.org/10.1016/j.postharvbio.2017.12.011.

Fan, K., Li, X., Cao, Y., Qi, H., Li, L., Zhang, Q., Sun, H., 2015. Carvacrol inhibits proliferation and induces apoptosis in human colon cancer cells. Anti Canccer Drugs 26, 813–823. https://doi.org/10.1097/CAD.0000000000000263.

Felgueiras, J., Silva, J.V., Fardilha, M., 2014. Prostate cancer: the need for biomarkers and new therapeutic targets. J. Zhejiang Univ. - Sci. B 15, 16–42. https://doi.org/10.1631/jzus.B1300106.

Gigliotti, C.L., Minelli, R., Cavalli, R., Occhipinti, S., Barrera, G., Pizzimenti, S., Cappellano, G., Boggio, E., Conti, L., Fantozzi, R., Giovarelli, M., Trotta, F., Dianzani, U., Dianzani, C., 2016. *In vitro* and *in vivo* therapeutic evaluation of camptothecin-encapsulated β-cyclodextrin nanosponges in prostate cancer. J. Biomed. Nanotechnol. 12, 114–127. https://doi.org/10.1166/jbn.2016.2144.

Guimarães, A.G., Oliveira, G.F., Melo, M.S., Cavalcanti, S.C.H., Antoniolli, A.R., Bonjardim, L.R., Silva, F.A., Santos, J.P.A., Rocha, R.F., Moreira, J.C.F., Araújo, A.A.S., Gelain, D.P., Quintans-Júnior, L.J., 2010. Bioassay-guided evaluation of antioxidant and antinociceptive activities of carvacrol. Basic Clin. Pharmacol. Toxicol. 107, 949–957. https://doi.org/10.1111/j.1742-7843.2010.00609.x.

Guimarães, A.G., Oliveira, M.A., Alves, R.D.S., Menezes, P.D.P., Serafini, M.R., De Souza Araújo, A.A., Bezerra, D.P., Quintans, L.J., 2015. Encapsulation of carvacrol, a monoterpene present in the essential oil of oregano, with β-cyclodextrin, improves the pharmacological response on cancer pain experimental protocols. Chem. Biol. Interact. 227, 69–76. https://doi.org/10.1016/j.cbi.2014.12.020.

Guimarães, A.G., Xavier, M.A., De Santana, M.T., Camargo, E.A., Santos, C.A., Brito, F.A., Barreto, E.O., Cavalcanti, S.C.H., Antoniolli, Â.R., Oliveira, R.C.M., Quintans-Júnior, L.J., 2012. Carvacrol attenuates mechanical hypernociception and inflammatory response. Naunyn-Schmiedeberg's Arch. Pharmacol. 385, 253–263. https://doi.org/10.1007/s00210-011-0715-x.

Günes-Bayir, A., Kocyigit, A., Güler, E.M., Bilgin, M.G., Ergün, İ.S., Dadak, A., 2018. Effects of carvacrol on human fibroblast (WS-1) and gastric adenocarcinoma (AGS) cells *in vitro* and on Wistar rats *in vivo*. Mol. Cell. Biochem. 0, 1–13. https://doi.org/10.1007/s11010-018-3329-5.

Gupta, S., 2007. Prostate cancer chemoprevention: Current status and future prospects. Toxicol. Appl. Pharmacol. 224, 369–376. https://doi.org/10.1016/j.taap.2006.11.008.

Hădărugă, N.G., 2012. Ficaria verna Huds. extracts and their β-cyclodextrin supramolecular systems. Chem. Cent. J. 6, 399. https://doi.org/10.1186/1752-153X-6-16.

Hill, L.E., Gomes, C., Taylor, T.M., 2013. Characterization of beta-cyclodextrin inclusion complexes containing essential oils (*trans*-cinnamaldehyde, eugenol, cinnamon bark, and clove bud extracts) for antimicrobial delivery applications. LWT - Food Sci. Technol. 51, 86–93. https://doi.org/10.1016/j.lwt.2012.11.011.

Iqbal, J., Abbasi, B.A., Mahmood, T., Kanwal, S., Ali, B., Shah, S.A., Khalil, A.T., 2017. Plant-derived anticancer agents: A green anticancer approach. Asian Pac. J. Trop. Biomed. 7, 1129–1150. https://doi.org/10.1016/j.apjtb.2017.10.016.

Kaur, V., Kumar, M., Kumar, A., Kaur, K., Dhillon, V.S., Kaur, S., 2017. Pharmacotherapeutic potential of phytochemicals: Implications in cancer chemoprevention and future perspectives. Biomed. Pharmacother. 97, 564–586. https://doi.org/10.1016/j.biopha.2017.10.124.

Kfoury, M., Lounès-Hadj Sahraoui, A., Bourdon, N., Laruelle, F., Fontaine, J., Auezova, L., Greige-Gerges, H., Fourmentin, S., 2016. Solubility, photostability and antifungal activity of phenylpropanoids encapsulated in cyclodextrins. Food Chem. 196, 518–525. https://doi.org/10.1016/j.foodchem.2015.09.078.

Kim, S.H., Bae, H.C., Park, E.J., Lee, C.R., Kim, B.J., Lee, S., Park, H.H., Kim, S.J., So, I., Kim, T.W., Jeon, J.H., 2011. Geraniol inhibits prostate cancer growth by targeting cell cycle and apoptosis pathways. Biochem. Biophys. Res. Commun. 407, 129–134. https://doi.org/10.1016/j.bbrc.2011.02.124.

Koparal, A.T., Zeytinoglu, M., 2003. Effects of carvacrol on a human non-small cell lung cancer (NSCLC) cell line, A549. Cytotechnology 43, 149–154.

Kurkov, S.V., Loftsson, T., 2013. Cyclodextrins. Int. J. Pharm. 453, 167–180. https://doi.org/10.1016/j.ijpharm.2012.06.055.

Luo, Y., Wu, J., Lu, M., Shi, Z., Na, N., Di, J., 2016. Carvacrol alleviates prostate cancer cell proliferation, migration, and invasion through regulation of PI3K/Akt and MAPK signaling pathways. Oxid. Med. Cell. Longev. 2016, 1–11. https://doi.org/10.1155/2016/1469693.

Marreto, R.N., Almeida, E.E.C.V., Alves, P.B., Niculau, E.S., Nunes, R.S., Matos, C.R.S., Araújo, A.A.S., 2008. Thermal analysis and gas chromatography coupled mass spectrometry analyses of hydroxypropyl-β-cyclodextrin inclusion complex containing *Lippia gracilis* essential oil. Thermochim. Acta 475, 53–58. https://doi.org/10.1016/j.tca.2008.06.015.

Melo, F.H.C., Rios, E.R.V., Rocha, N.F.M., Citó, M., do, C., de, O., Fernandes, M.L., de Sousa, D.P., de Vasconcelos, S.M.M., de Sousa, F.C.F., 2012. Antinociceptive activity of carvacrol (5-isopropyl-2-methylphenol) in mice. J. Pharm. Pharmacol. 64, 1722–1729. https://doi.org/10.1111/j.2042-7158.2012.01552.x.

Menezes, P. dos P., Dória, G.A.A., de Souza Araújo, A.A., Sousa, B.M.H., Quintans-Júnior, L.J., Lima, R.N., Alves, P.B., Carvalho, F.M.S., Bezerra, D.P., Mendonça-Júnior, F.J.B., Scotti, L., Scotti, M.T., da Silva, G.F., de Aquino, T.M., Sabino, A.R., do Egito, E.S.T., Serafini, M.R., 2016. Docking and physico-chemical properties of α- and β-cyclodextrin complex containing isopulegol: a comparative study. J. Inclusion Phenom. Macrocycl. Chem. 85, 341–354. https://doi.org/10.1007/s10847-016-0633-0.

Mura, P., 2015. Analytical techniques for characterization of cyclodextrin complexes in the solid state: A review. J. Pharmaceut. Biomed. Anal. 113, 226–238. https://doi.org/10.1016/j.jpba.2015.01.058.

Nichol, J.W., Koshy, S.T., Bae, H., Hwang, C.M., Yamanlar, S., Khademhosseini, A., 2010. Cell-laden microengineered gelatin methacrylate hydrogels. Biomaterials 31, 5536–5544. https://doi.org/10.1016/j.biomaterials.2010.03.064.

Oliveira, M.G.B., Brito, R.G., Santos, P.L., Araújo-Filho, H.G., Quintans, J.S.S., Menezes, P.P., Serafini, M.R., Carvalho, Y.M.B.G., Silva, J.C., Almeida, J.R.G.S., Scotti, L., Scotti, M.T., Shanmugam, S., Thangaraj, P., Araújo, A.A.S., Quintans-Júnior, L.J., 2016. α-Terpineol, a monoterpene alcohol, complexed with β-cyclodextrin exerts antihyperalgesic effect in animal model for fibromyalgia aided with docking study. Chem. Biol. Interact. 254, 54–62. https://doi.org/10.1016/j.cbi.2016.05.029.

Rejhová, A., Opattová, A., Čumová, A., Slíva, D., Vodička, P., 2018. Natural compounds and combination therapy in colorectal cancer treatment. Eur. J. Med. Chem. 144, 582–594. https://doi.org/10.1016/j.ejmech.2017.12.039.

Santos, E.H., Kamimura, J. a., Hill, L.E., Gomes, C.L., 2015. Characterization of carvacrol beta-cyclodextrin inclusion complexes as delivery systems for antibacterial and antioxidant applications. LWT - Food Sci. Technol. 60, 583–592. https://doi.org/10.1016/j.lwt.2014.08.046.

Santos, P.L., Brito, R.G., Oliveira, M.A., Quintans, J.S.S., Guimarães, A.G., Santos, M.R.V., Menezes, P.P., Serafini, M.R., Menezes, I.R.A., Coutinho, H.D.M., Araújo, A.A.S., Quintans-Júnior, L.J., 2016. Docking, characterization and investigation of β-cyclodextrin complexed with citronellal, a monoterpene present in the essential oil of *Cymbopogon* species, as an anti-hyperalgesic agent in chronic muscle pain model. Phytomedicine 23, 948–957. https://doi.org/10.1016/j.phymed.2016.06.007.

Siegel, R.L., Miller, K.D., Jemal, A., 2018. Cancer statistics, 2018. Ca. Canc. J. Clin. 68, 7–30. https://doi.org/10.3322/caac.21442.

Souza, M.T. de S., Teixeira, D.F., de Oliveira, J.P., Oliveira, A.S., Quintans-Júnior, L.J., Correa, C.B., Camargo, E.A., 2017. Protective effect of carvacrol on acetic acid-induced colitis. Biomed. Pharmacother. 96, 313–319. https://doi.org/10.1016/j.biopha.2017.10.017.

Su, J., Chen, J., Li, L., Li, B., Shi, L., Zhang, H., Ding, X., 2012. Preparation of natural borneol/2-hydroxypropyl-β-cyclodextrin inclusion complex and its effect on the absorption of tetramethylpyrazine phosphate in mouse. Chem. Pharm. Bull. (Tokyo) 60, 736–742. https://doi.org/10.1248/cpb.60.736.

Szente, L., Szejtli, J., 2004. Cyclodextrins as food ingredients. Trends Food Sci. Technol. 15, 137–142. https://doi.org/10.1016/j.tifs.2003.09.019.

Wang, X., Luo, Z., Xiao, Z., 2014. Preparation, characterization, and thermal stability of β-cyclodextrin/soybean lecithin inclusion complex. Carbohydr. Polym. 101, 1027–1032. https://doi.org/10.1016/j.carbpol.2013.10.042.

Wang, Y., Wang, X., Yang, Z., Zhu, G., Chen, D., Meng, Z., 2012. Menthol inhibits the proliferation and motility of prostate cancer DU145 Cells. Pathol. Oncol. Res. 18, 903–910. https://doi.org/10.1007/s12253-012-9520-1.

Yallapu, M.M., Jaggi, M., Chauhan, S.C., 2010. β-Cyclodextrin-curcumin self-assembly enhances curcumin delivery in prostate cancer cells. Colloids Surfaces B Biointerfaces 79, 113–125. https://doi.org/10.1016/j.colsurfb.2010.03.039.

Yildiz, Z.I., Celebioglu, A., Kilic, M.E., Durgun, E., Uyar, T., 2018. Fast-dissolving

carvacrol/cyclodextrin inclusion complex electrospun fibers with enhanced thermal stability, water solubility, and antioxidant activity. J. Mater. Sci. 53, 15837–15849. https://doi.org/10.1007/s10853-018-2750-1.

Yin, Q., Yan, F., Zu, X.-Y., Wu, Y., Wu, X., Liao, M., Deng, S., Yin, L., Zhuang, Y., 2012. Anti-proliferative and pro-apoptotic effect of carvacrol on human hepatocellular carcinoma cell line HepG-2. Cytotechnology 64, 43–51. https://doi.org/10.1007/s10616-011-9389-y.

Zhao, Y., Chen, R., Wang, Y., Qing, C., Wang, W., Yang, Y., 2017. *In vitro* and *in vivo* Efficacy Studies of *Lavender angustifolia* Essential Oil and Its Active Constituents on the Proliferation of Human Prostate Cancer. Integr. Canc. Ther. 16, 215–226. https://doi.org/10.1177/1534735416645408.